DOI: http://dx.doi.org/10.22104/jpst.2015.75

Journal of Particle Science and Technology (2015) 21-30

Journal of Particle Science and Technology

J | P | S | T

jpst.irost.ir

Preparation of Gd_2O_3 nanoparticles from a new precursor and their catalytic activity for electrochemical reduction of CO_2 to CO

Mohammad Taghi Behnamfar [1,*]

[1] *Department of Chemistry, Isfahan University of Technology, Isfahan 84156-83111, Iran*

HIGHLIGHTS

- A new Gd(III) complex has been prepared and characterized.
- The Gd_2O_3 nanoparticles were prepared from Gd(III) complex precipitates.
- Electrochemical reduction of CO_2 to CO was studied in the presence of compounds.
- The Gd(III) complex and Gd_2O_3 nanoparticles can catalyze the electrochemical reduction of CO_2 to CO.

GRAPHICALABSTRACT

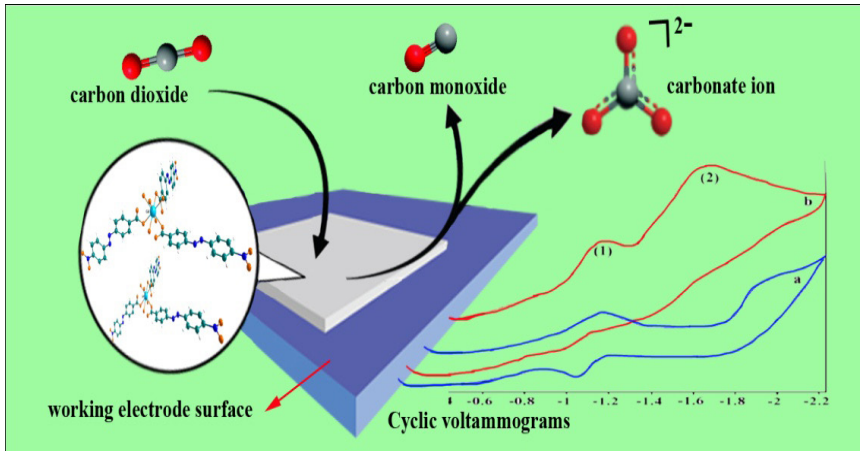

ARTICLE INFO

Article history:
Received 22 November 2014
Received in revised form
3 December 2014
Accepted 6 December 2014

Keywords:
Gd(III) complex
Gd_2O_3 nanoparticles
CO_2 reduction
Cyclic voltammetry
alizarin yellow R

ABSTRACT

The mononuclear Gd(III) complex, $[Gd(L)_3(H_2O)_5]$ (where L is alizarin yellow R ($NaC_{13}H_8N_3O_5$)), has been prepared in H_2O under reflux condition. The Gd(III) complex has been characterized by elemental analysis and spectroscopic methods (UV–Vis and FT–IR). The Gd_2O_3 nanoparticles were prepared by the calcination of the Gd(III) complex in air at different temperatures up to 600 °C for 2 h. The calcination temperature was the key parameter which was changed for more investigation. The products were characterized by various methods such as FT–IR, X-ray diffraction analysis and field-emission scanning electron microscopy (FE–SEM). The electrochemical studies of the Gd(III) complex and Gd_2O_3 nanoparticles were performed in acetonitrile. The voltammograms in the absence and presence of carbon dioxide indicate that $[Gd(L)_3(H_2O)_5]$ and Gd_2O_3 nanoparticles can catalyze the electrochemical reduction of CO_2 to CO.

*Corresponding author. Tel.: +98 311 3913240; fax: +98 311 3912350.
E-mail address: mt.behnamfar@ch.iut.ac.ir, behnam10@gmail.com (MT.Behnamfar).

1. Introduction

Carbon dioxide is an important greenhouse gas produced by human activities, primarily through the combustion of fossil fuels; however, methane, chlorofluorocarbons and other gases are more potent greenhouse gases. Its concentration in the Earth's atmosphere has risen by more than 35% since the Industrial Revolution. Atmospheric mixing ratios for carbon dioxide are now higher than at any time in at least the last 800,000 years, standing at 385 parts per million (ppm) compared to a pre-industrial high of 280 ppm. The current rate of increase is around two ppm per year. This rate has caused much worry in the international community. Therefore, the fixation of CO_2 and conversion into a useful chemical feedstock is of potential benefit. Research in the field of electrochemical reduction of CO_2 has grown rapidly in the last few decades. This growing research effort is a response by physical scientists and engineers to the increasing amount of CO_2 in the atmosphere and the steady growth in global fuel demand. Electrochemical reduction of CO_2 with metal complexes is a feasible technique for the utilization of CO_2 as a C_1 source, though the reduction products usually have been limited to CO and/or HCOOH. Metal complexes with η^1–CO_2 are considered to play the key role in the reduction of CO_2, since metal—η^1–CO_2 is easily converted to metal—CO through an acid–base reaction in protic media or via oxide transfer to free CO_2 in aprotic media. CO evolution in the reduction of CO_2 is ascribed to reductive cleavage of the resulting metal—CO [1–14].

Nanoparticles have emerged as sustainable alternatives to conventional materials, as robust, high surface area heterogeneous catalysts and catalyst supports. The nano-sized particles increase the exposed surface area of the active component of the catalyst, thereby enhancing the contact between reactants and catalyst dramatically and mimicking the homogeneous catalysts. However, their insolubility in reaction solvents renders them easily separable from the reaction mixture like heterogeneous catalysts, which in turn makes the product isolation stage effortless. Also, the activity and selectivity of nano-catalyst can be manipulated by tailoring chemical and physical properties like size, shape, composition and morphology. The scientific challenge is the synthesis of specific-size and shape nano-catalysts to allow facile movement of materials in the reacting phase and control over morphology of nanostructures to tailor their physical and chemical properties. However, the rapid advancement of nano-technology made possible the preparation of a variety of nanoparticles with controlled size, shape, morphology and composition [15–25].

Here, I report the synthesis and characterization of a new mononuclear Gd(III) complex, $[Gd(L)_3(H_2O)_5]$ where L is alizarin yellow R (Fig. 1). A simple method is reported for the preparation of the Gd_2O_3 nanoparticles from a new precursor complex by a facile calcination method. The electrocatalytic reduction of CO_2 to CO by the complex and Gd_2O_3 nanoparticles was investigated using cyclic voltammetry (CV) in CH_3CN-solution.

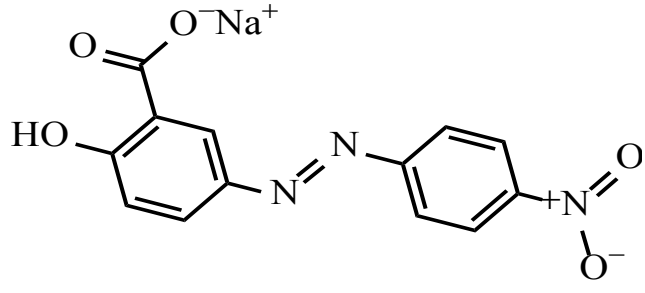

Fig. 1. Molecular structure of alizarine yellow R.

2. Experimental

2.1. Materials and Methods

$GdCl_3{\cdot}6H_2O$, alizarin yellow R, tetra-*n*-butylammonium hexafluorophosphate and acetonitrile were purchased from Merck. Deionized water was used to wash all nanoparticles. All chemicals and solvents were of high purity and used without any further purification.

Elemental analysis (C, H and N) were performed by using a Leco, CHNS-932 elemental analyzer. Fourier transform infrared spectra were recorded on an FT-IR JASCO 680-PLUS spectrometer in the region of 4000–400 cm^{-1} using KBr pellets. Electronic absorption spectra were recorded on a JASCO 7580 UV–Vis–NIR double-beam spectrophotometer using quartz cells with a path length of 10 mm. The XRD analyses were performed using the X-ray diffractometer (PHILIPS PW3040/60) with Cu*Ka* radiation. The morphology of the nanoparticles was observed using FE-SEM (HITACHI; S-4160). Voltammetric experiments were performed on a SAMA Research Analyzer M-500. All measurements were carried out in a 5 mL cell which was fitted with a Teflon lid incorporating a three-electrode system comprising of a glassy carbon electrode (ϕ = 2 mm) as the working electrode, a platinum wire as the auxiliary electrode and a silver wire as the pseudo-reference electrode

(the potential values reported versus SCE). The glassy carbon working electrode surface was freshly cleaned with alumina polish on a micro cloth before each scan and was rinsed with doubly-distilled water between each polishing step. Cyclic voltammetry of an acetonitrile solution of $[Gd(L)_3(H_2O)_5]$ was carried out with a 0.1 M solution of tetra-*n*-butylammoniumhexafluorophosphate (TBAH) as the supporting electrolyte. Fer rocene (E° = 0.665 V vs. NHE) was used as an internal reference at the end of each experiment. The solutions were purged by N_2 or CO_2 flows during study. All spectral and electrochemical data were collected at ambient temperature.

2.2. Synthesis of $[Gd(L)_3(H_2O)_5]$

The $[Gd(L)_3(H_2O)_5]$ (L = alizarin yellow R) complex was synthesis by the reaction of alizarin yellow R and gadolinium(III) chloride hexahydrate in 30 mL water. Alizarin yellow R (0.93 g, 3 mmol) was dissolved in 15 mL of water under stirring at 80°C until a dark yellow solution resulted To the solution was then added a solution of $GdCl_3{\cdot}6H_2O$ (0.37 g, 1 mmol) in 15 mL water. The reaction mixture was refluxed for 5 h. The orange precipitate was filtered and washed with water and dried in air at room temperature (scheme. 1). Yield: 0.92 g, 83%. Anal. Calc. for $GdC_{39}H_{34}N_9O_{20}$ (MW = 1105.99 g/mol): C, 42.35; H, 3.10; N, 11.40 % Found: C, 42.51; H, 3.18; N, 11.58%.

2.3. Synthesis of Gd_2O_3 nanoparticles

The precursor Gd(III) complex was prepared by calcination up to 600°C.Brown gadolinium oxide nanoparticles were produced by subjecting 0.3 mg of the as-prepared Gd(III) complex powder to heat treatment at a relatively low temperature (300 °C) in air. An average temperature increase of 20 °C every minute was selected before the temperature reached 300 °C, and after keeping the thermal treatment at 300 °C for 2 h, it was allowed to cool to room temperature naturally. A series of further experiments were carried out to investigate the reaction conditions. Detailed reaction conditions and the corresponding results are summarized in Table 1.

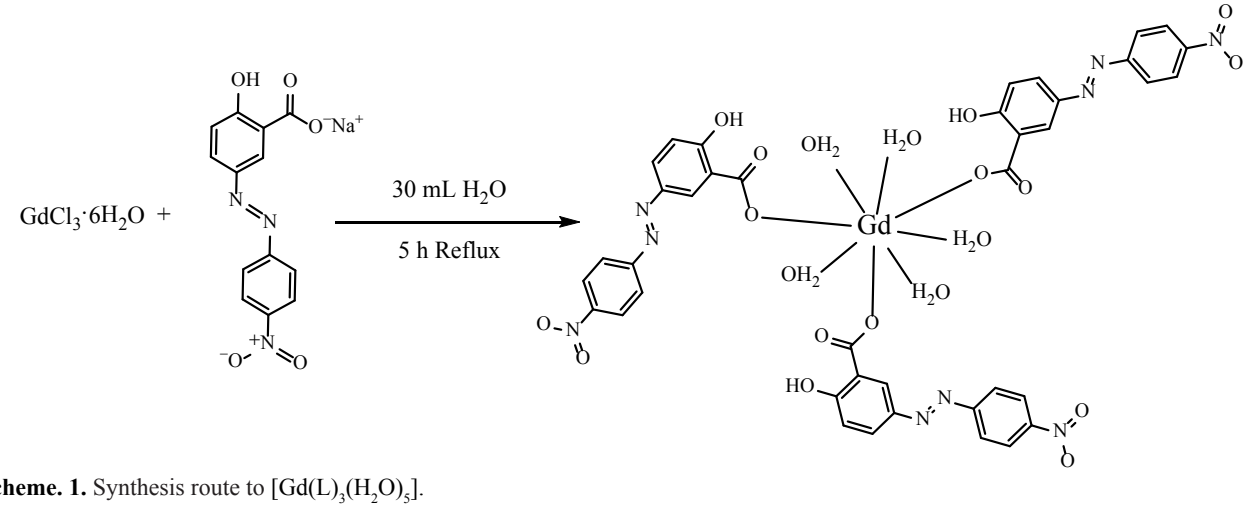

Scheme. 1. Synthesis route to $[Gd(L)_3(H_2O)_5]$.

Table. 1.
Products obtained under different calcination conditions.

Sample no.	Calcinations' temperature (°C)	Calcinations' time (h)	Average size of nanoparticles	Morphologies of the products	Figures' no.
1	300	2	10 µm	nanoparticle	Fig. 6, a and b
2	400	2	15 nm	nanoparticle	Fig. 6, c and d
3	500	2	15 nm	nanoparticle	Fig. 7, e and f
4	600	2	150 nm	nanoflake	Fig. 7, g and h

3. Results and discussion

3.1. Synthesis and characterization of $[Gd(L)_3(H_2O)_5]$

The reaction of alizarin yellow R with $DyCl_3 \cdot 6H_2O$ is shown in Scheme 1. The complex was prepared in good yield. The elemental analyze of the complex was entirely consistent with their proposed composition. Fig. 2 shows the optimized structure of $[Gd(L)_3(H_2O)_5]$. According to Fig. 2, the binding of alizarin ligands to gadolinium, causing the tripodal-like complex.

3.2. UV–Vis and FT-IR spectroscopic studies

To obtain suitable electronic absorption spectrum, the complex was dissolved in acetonitrile. The complex demonstrate three absorption bands in the UV–Vis region (200–700 nm) that can be assigned to ligand-centered ($\pi \rightarrow \pi^*$ and $n \rightarrow \pi^*$) transitions [26].

The orange color observed for Gd(III) complex can be attributed to appearance of some of the $n \rightarrow \pi^*$ transitions that overlap with more energetic transitions and thus the sequence of absorption spectrum has been expanded to visible region.

The FT-IR spectra of the pure alizarin yellow R, $[Gd(L)_3(H_2O)_5]$ complex and Gd_2O_3 nanoparticles recorded as KBr disk and shown in Fig. 4. In the IR spectrum of $[Gd(L)_3(H_2O)_5]$, the bands associated with the carbonyl stretching are clearly seen. By comparison of the spectra of $[Gd(L)_3(H_2O)_5]$ with the free alizarin yellow R ligand, it is determined that the bands at about 1670 cm^{-1} are carbonyl stretching vibrations in the coordinated alizarin yellow R ligand [27]. The absorption peaks at 3445 and 1633cm^{-1} is attributed to the stretching vibration of the O–H bond and the bending vibration of H–O–H from water. The absorption band of Gd–O appears at 550 cm^{-1} and 433 cm^{-1}. In the IR spectrum of Gd_2O_3 nanoparticles, the bands associated with the Gd–O vibrations are appear at 546 and 431 cm^{-1} [27,28].

3.3. FE-SEM studies

The morphological images of gadolinium oxide nanoparticles were obtained by FE-SEM. Some conditions were examined to investigate the morphology of products (table. 1), if any, and compare them with each other. Fig.6 and 7 shows FE-SEM images of the gadolinium oxide nanoparticles calcined at 300 °C (sample no. 1, Fig. 6, a and b), 400 °C (sample no. 2, Fig. 6, c and d), 500 °C (sample no. 3, Fig. 7, e and f), and 600 °C (sample no. 4, Fig. 7, g and h) for 2 h, respectively. At 300 °C some parts of organic matters are remaining and nanoparticles have not yet formed. Quasi-spherical nanoparticles are observed when the calcinations temperature is between 400 and 500 °C. At 600 °C, the particles grow up and have been sintered together leading to the formation of nanoflake. The images show that with increasing of calcination temperature, the size of the nanoparticles become larger. According to the FE-SEM results, the particle size of the Gd_2O_3 nanoparticles (sample no. 2 and 3) are between 10 and 20 nm.

3.4. XRD analysis

XRD analysis, which is the most useful technique for identification of crystalline structure, was employed to investigate the prepared sample. The X-ray diffraction pattern of Gd_2O_3 nanoparticles was shown in Fig. 5. The diffraction patterns show that nanoparticles have a crystalline morphology and haven't any amorphous phase at their structures. In Fig. 5, the X-ray diffraction pattern of sample no. 3 is shown. Calcination of $[Gd(L)_3(H_2O)_5]$ at a three temperatures (400°C, 500°C and 600 °C) resulted the crystalline phase, namely gadolinium oxide (Fig. 6, c, d and Fig. 7), which is in agreement with that have been reported [28,29]. As shown in Fig. 5 the XRD pattern of the pure Gd_2O_3 reveals that the diffractogram can be deter-

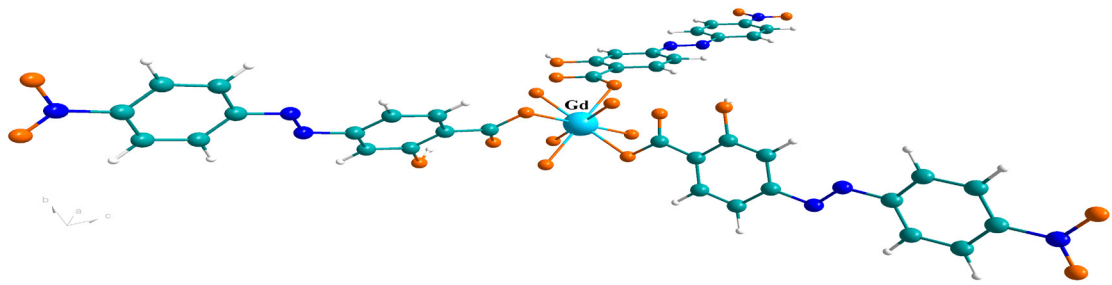

Fig. 2. The optimized structure of $[Gd(L)_3(H_2O)_5]$.

mined as Gd_2O_3 with cubic phase, which can be filed to (222), (400), (440), (622), (662) and (844) planes (JCPDS Card No. 011- 0608). From XRD data Fig. 5, the crystallite size (Dc) of the Gd_2O_3, sample no. 3, was calculated to be 15 nm using the Debey-Scherrer equation[30],

$$D_c = K\lambda / \beta cos\theta$$

where β is the breadth of the observed diffraction line at its half maximum intensity, K is the so-called shape factor, which usually takes a value of about 0.9, and λ is the wavelength of X-ray source used in XRD. The average size of the particles of sample no. 3, was 15 nm, which is to some extent in agreement with that observed from FE-SEM images.

3.5. Electrocatalytic activity

To study the electrocatalytic activity of the compounds ($[Gd(L)_3(H_2O)_5]$ and sample no. 3) in the CO_2 reduction, cyclic voltammograms of the compounds under a flow of carbon dioxide were taken and compared with those obtained under a nitrogen atmosphere. In the case of complex a precatalyst solution was prepared by dissolving 5 mg of the complex in 5 mL of electrolyte solution (0.1 M TBAH in acetonitrile) to give a concentration of ca. 1 mM. And also in the case of nanoparticles a precatalyst was prepared by dispersing 2 mg of the nanoparticles in 1 mL of water and deposited 10 µL of dispersed nanoparticles on the GC electrode surface. 0.1 M TBAH in acetonitrile was used for electrolyte solution. The voltammetric response of the complex under two different nitrogen and carbon dioxide gas blowing mode will be briefly discussed here.

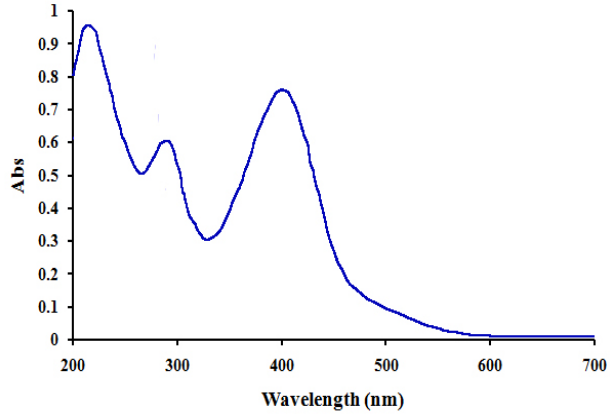

Fig. 3. Electronic spectrum of $[Gd(L)_3(H_2O)_5]$ (1×10^{-5} M) in H_2O.

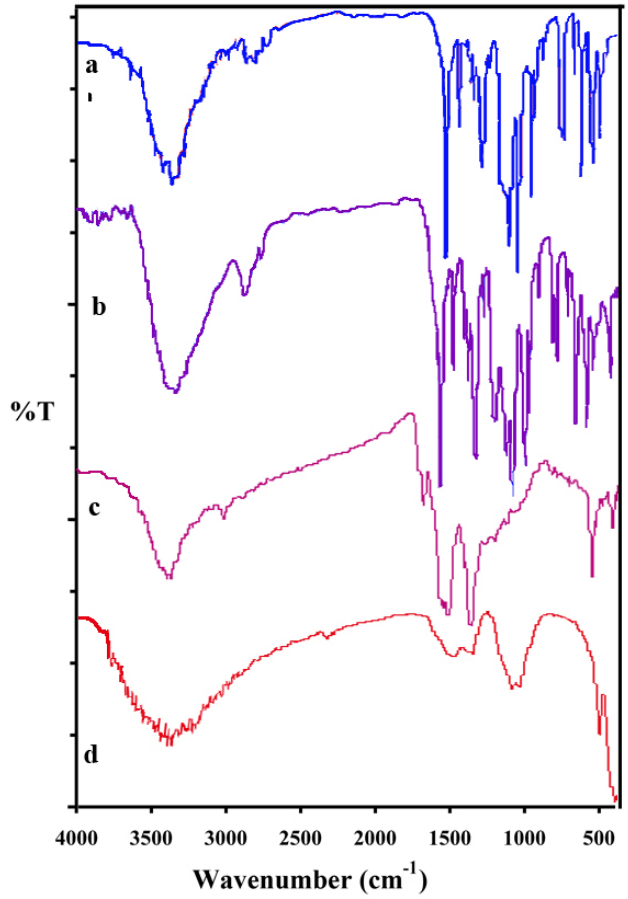

Fig. 4. FT-IR spectra of a) alizarine yellow R, b) $[Gd(L)_3(H_2O)_5]$, c) sample no. 1 and d) sample no. 3.

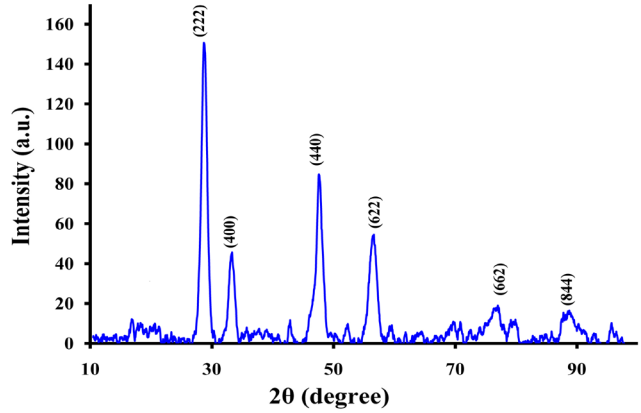

Fig. 5. XRD patterns of Gd_2O_3 nanoparticles calcined at 500 °C (sample no. 3).

3.5.1 Electrochemical study under N2 atmosphere

The cyclic voltammograms of the complex and nanoparticles (sample no. 3) at a glassy carbon (GC) electrode are shown in Fig. 8, a, and Fig. 9, a. Cyclic voltammetry measurements were performed on an acetonitrile solution of the complex with 0.1 M TBAH

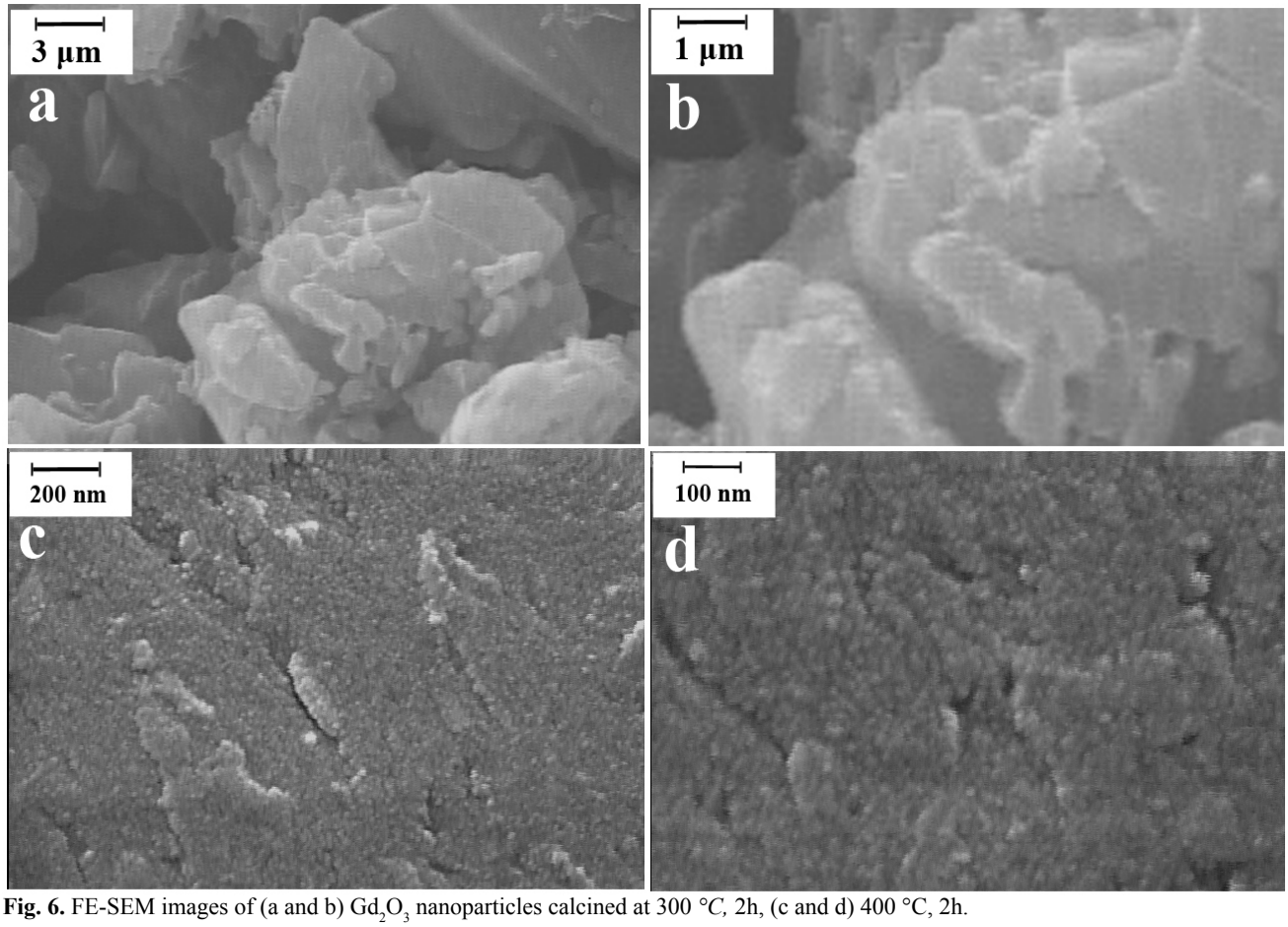

Fig. 6. FE-SEM images of (a and b) Gd_2O_3 nanoparticles calcined at 300 °*C,* 2h, (c and d) 400 °C, 2h.

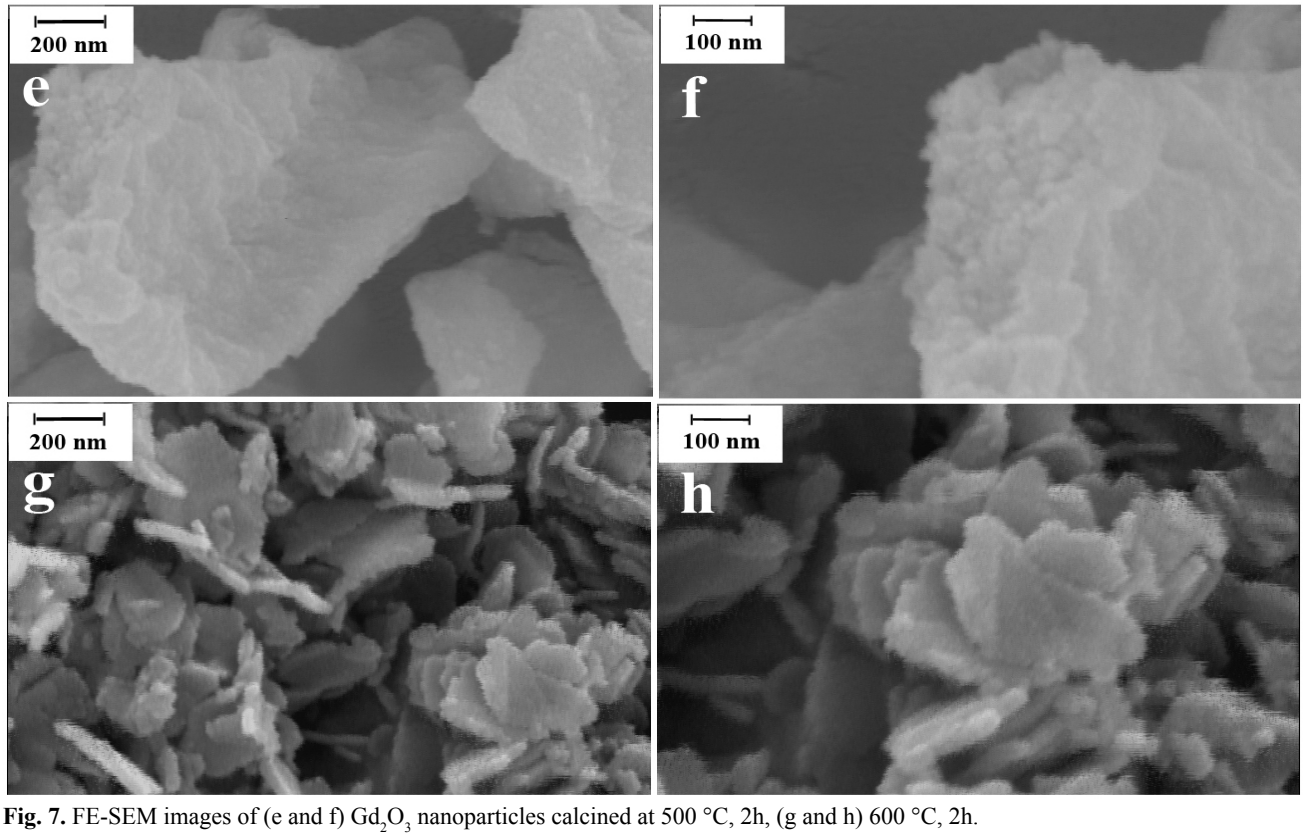

Fig. 7. FE-SEM images of (e and f) Gd_2O_3 nanoparticles calcined at 500 °C, 2h, (g and h) 600 °C, 2h.

supporting electrolyte at ambient temperature. The voltammogram recorded in N_2 present four couples at −1.18, −1.05, and −1.98 V versus SCE that assigned to the three alizarin yellow R couples and the Gd(III/II) reduction couple, respectively. The formal potential, $E_{1/2}$, was calculated from the average of the anodic and cathodic peak potentials, where $E_{1/2}$ = (Ep.a + Ep.c)/2 at a scan rate of 0.1 V s^{-1}. Under the N2 atmosphere, the alizarin yellow R couples exhibits equivalent anodic and cathodic waves, with 0.065 V peak separations. The irreversible reduction wave in the negative potential region is assigned to the reduction of the Gd(III/II) couple. In the case of nanoparticles (sample no. 3) the voltammogram recorded in N_2 present a Voltammetric peak at −2.17 V versus SCE that assigned to the irreversible Gd(III/II) reduction couple.

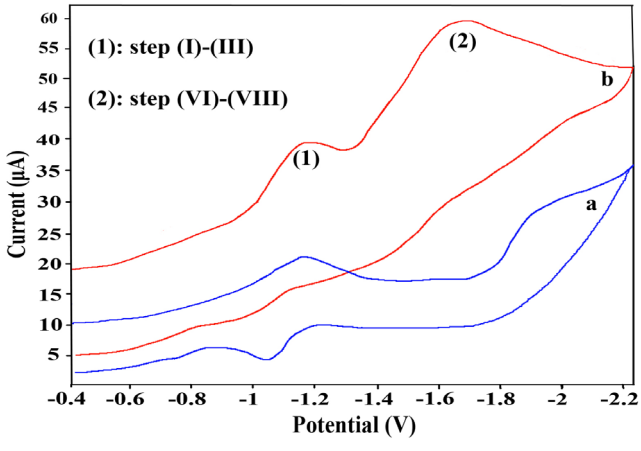

Fig. 8. Cyclic voltammograms of $[Gd(L)_3(H_2O)_5]$ (10^{-3}M) (a) in the absence and (b) presence of CO_2 at scan rate of 100 mV/s; in dry acetonitrile; 0.1 M TBAH.

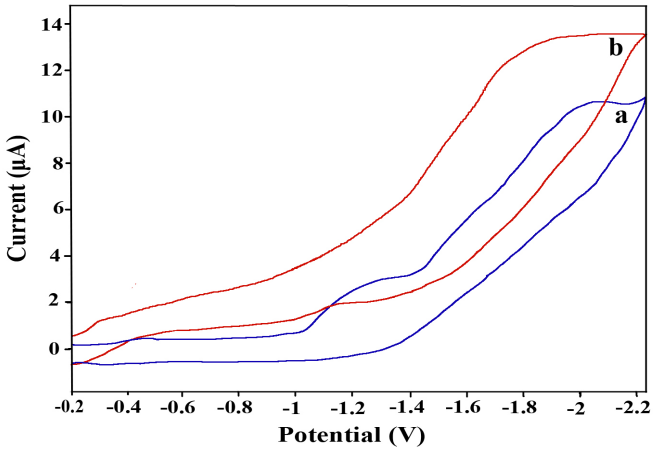

Fig. 9. Cyclic voltammograms of Gd_2O_3 nanoparticles (sample no. 3) (a) in the absence and (b) presence of CO_2 at scan rate of 100 mV/s; in dry acetonitrile; 0.1 M TBAH.

3.5.2 Electrochemical study under CO_2 atmosphere

Fig. 8, b, shows the cyclic voltammograms of a solution, purged by CO_2 flow, containing 1 mM of the complex in 0.1 M TBAH/CH_3CN at a glassy carbon electrode. Also Scheme. 2 shows the Proposed reaction mechanism for the electrocatalytic reduction of CO_2 by the Gd(III) complex. As can be seen in Fig. 8, b, some significant changes are observed when the N_2 atmosphere is replaced by CO_2. Around −1.20 V, one signal appears which can be assigned to the 1ē reductions that involve the each three alizarin ligands. In a solution saturated with CO_2, the reduction wave (1) is approximately unchanged with respect to an N_2-saturated solution (Fig. 8, b). The first, second and third one-electron reductions of $[Gd(L)_3(H_2O)_5]$ provide three electrons that enter the empty π* orbitals of the alizarin ligands. These observations are consistent with the alizarin-based reduction to give $[GdIII(L^{-\bullet})_3(H_2O)_5]^{3-}$ followed by reaction with CO_2, step (IV)(Scheme. 2). After the substitution of CO_2 with H_2O, an intramolecular two-electron transfer takes place from the alizarin to the coordinated CO_2 ligand to give an intermediate shown as the metallocarboxylate, promoting the reduction of CO_2. It may occur via an O^{2-} transfer to CO_2 to give CO_3^{2-} and a CO complex (step (VI)). In fact, the catalytic cycle needs two CO_2 molecules. One CO_2 is reduced to CO and another CO_2 is fixed to a carbonate anion. The carbonate anion (CO_3^{2-}) is stable and cannot convert to CO_2 in the experimental condition. There is a significant current enhancement for the wave at Ep.c = −1.67 V (wave (2) in Fig. 8, b), which consistent with the electrocatalytic reduction of CO_2 [2].

Fig. 9, b, shows the cyclic voltammograms of a precatalyst, purged by CO_2 flow, containing 10 μL of dispersed nanoparticles on the GC electrode surface in 0.1 M TBAH/CH_3CN. As can be seen in Fig. 9, b, some changes are observed when the N2 atmosphere is replaced by CO_2. A significant current enhancement for the wave at Ep.c = −1.88 V, can be assigned to the electrocatalytic reduction of CO_2.

4. Conclusions

Gd_2O_3 nanoparticles were prepared by the calcination of new Gd(III) complex precipitates in air at different temperatures up to 600 °C for 2 h. The products were characterized by various methods. The electrochemical studies of Gd complex and gadolinium

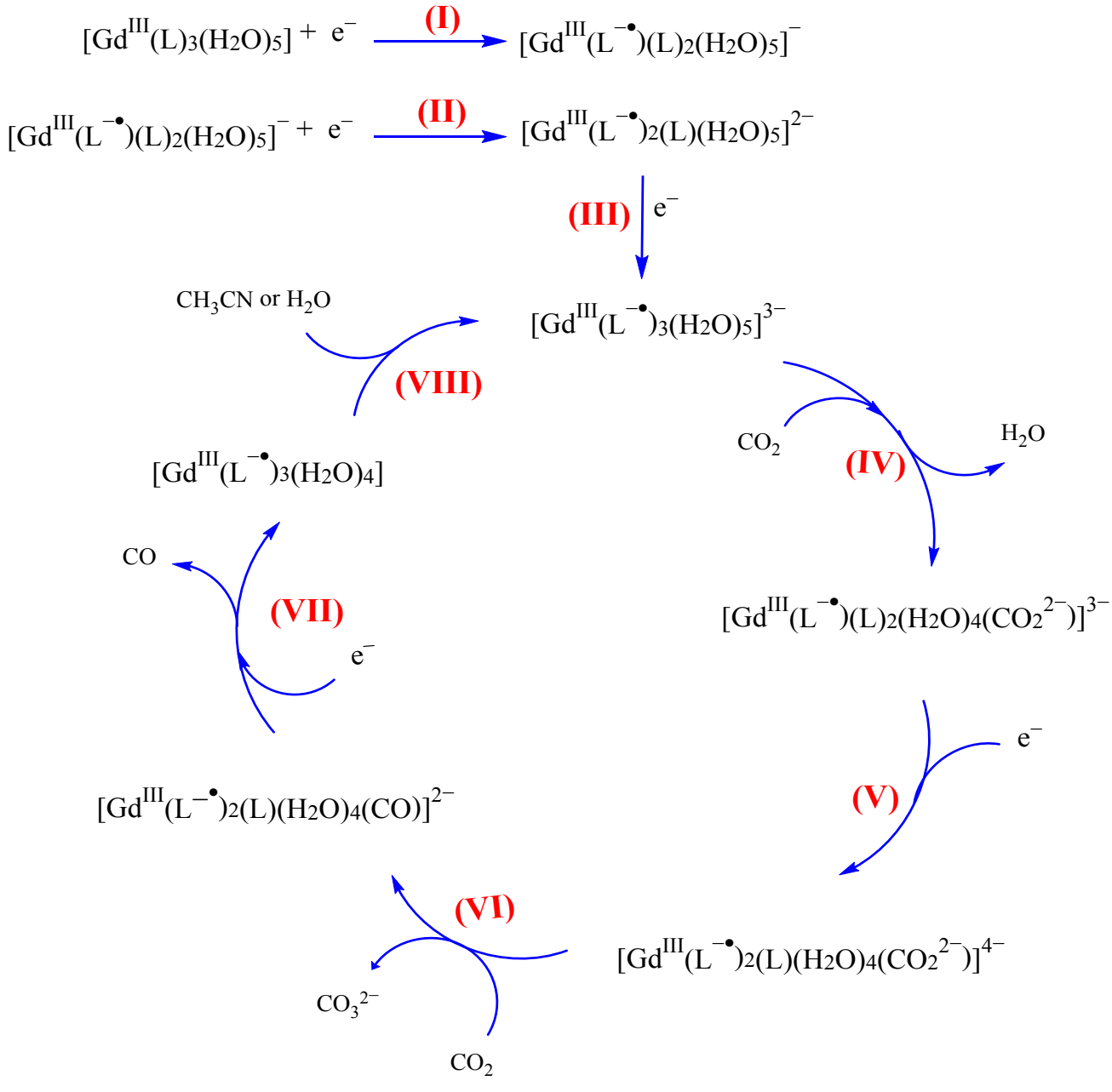

Scheme. 2. Proposed reaction mechanism for the electrocatalytic reduction of CO_2 by the Gd(III) complex in CH_3CN.

oxide nanoparticles were performed in acetonitrile. The voltammograms in the absence and presence of carbon dioxide indicates that the $[Gd(L)_3(H_2O)_5]$ and gadolinium oxide nanoparticles can catalyze the electrochemical reduction of CO_2 to CO.

Acknowledgements

I am grateful to the Isfahan University of Technology (IUT) for financial support.

References

[1]X. Frogneux, O. Jacquet, T. Cantat, Iron-catalyzed hydrosilylation of CO_2: CO_2 conversion to formamides and methylamines, Catal. Sci. Technol. 4 (2014) 1529.

[2]F.H. Haghighi, H. Hadadzadeh, H. Farrokhpour, N. Serri, K. Abdi, H. Amiri Rudbari, Computational and experimental study on the electrocatalytic reduction of CO_2 to CO by a new mononuclear ruthenium(ii) complex., Dalton Trans. 43 (2014) 11317–32.

[3]I. Knopf, T. Ono, M. Temprado, D. Tofan, C.C. Cummins, Uptake of one and two molecules of CO_2 by the molybdate dianion: a soluble, molecular oxide model system for carbon dioxide fixation, Chem. Sci. 5 (2014) 1772.

[4]B. Kumar, M. Llorente, J. Froehlich, T. Dang, A. Sathrum, C.P. Kubiak, Photochemical and photoelectrochemical reduction of CO_2., Annu. Rev. Phys. Chem. 63 (2012) 541–69.

[5]T. Mizukawa, K. Tsuge, H. Nakajima, K. Tanaka, Selective Production of Acetone in the Electrochemical Reduction of CO_2 Catalyzed by a Ru ± Naphthyridine Complex, Angew. Chem. Int. Ed. 38 (1999) 362–363.

[6]A.J. Morris, G.J. Meyer, E. Fujita, Molecular approaches to the photocatalytic reduction of carbon dioxide for solar fuels., Acc. Chem. Res. 42 (2009) 1983–94.

[7]I.M.B. Nielsen, K. Leung, Cobalt - Porphyrin Catalyzed Electrochemical Reduction of Carbon Dioxide in Water . 1 . A Density Functional Study of Intermediates, J. Phys. Chem. A,. 114 (2010) 10166–10173.

[8]R. Ortiz, C. Guti, FTIR spectroscopy study of the electrochemical reduction of on various metal electrodes in methanol, J. Electroanal. Chem. 390 (1995) 99–107.

[9]B.B.P. Sullivan, Reduction of Carbon Dioxide with Platinum Metals Electrocatalysts, Platin. Met. Rev. 33 (1989) 2–9.

[10]L. Sun, G.K. Ramesha, P. V Kamat, J.F. Brennecke, Switching the reaction course of electrochemical CO_2 reduction with ionic liquids., Langmuir. 30 (2014) 6302–8.

[11]K. Tanaka, T. Mizukawa, Selective formation of ketones by electrochemical reduction of CO_2 catalyzed by, Appl. Organometal. Chem. 866 (2000) 863–866.

[12]Z. Thammavongsy, T. Seda, L.N. Zakharov, W. Kaminsky, J.D. Gilbertson, Ligand-based reduction of CO_2 and release of CO on iron(II)., Inorg. Chem. 51 (2012) 9168–70.

[13]D.T. Whipple, P.J. a. Kenis, Prospects of CO_2 Utilization via Direct Heterogeneous Electrochemical Reduction, J. Phys. Chem. Lett. 1 (2010) 3451–3458.

[14]X. Zhang, Mechanism of CO_2 Activation by (PNN) Ru(H)(CO) Complex, Commun. Comput. Chem. 1 (2013) 191–203.

[15]introduction to nanocatalyst, (n.d.). http://rgn.krict.re.kr/index.sko.menuCd=BB02001002001.

[16]W. Zhang, K. Gilstrap, L. Wu, R.B.K. C, M.A. Moss, Q. Wang, et al., Synthesis and Characterization of Thermally Responsive Pluronic F127 Chitosan Nanocapsules for Controlled Release and Intracellular Delivery of Small Molecules, ACS Nano. 4 (2010) 6747–6759.

[17]C. Wen, D. Dunbar, X. Zhang, J. Lauterbach, J. Hattrick-Simpers, Self-healing catalysts: Co_3O_4 nanorods for Fischer-Tropsch synthesis., Chem. Commun. (Camb). 50 (2014) 4575–8.

[18]S. Ryoo, Y. Kim, M. Kim, D. Min, Behaviors of NIH-3T3 Fibroblasts on Graphene/Carbon Nanotubes: Proliferation, Focal Adhesion, and Gene Transfection Studies, ACS Nano. 4 (2010) 6587–6598.

[19]V. Polshettiwar, R.S. Varma, Green chemistry by nano-catalysis, Green Chem. 12 (2010) 743.

[20]Y.H. Lee, G. Lee, J.H. Shim, S. Hwang, J. Kwak, K. Lee, Monodisperse PtRu Nanoalloy on Carbon as a High-Performance DMFC Catalyst, Chem. Mater. 18 (2006) 4209–4211.

[21]M.T. L. P. Mahesh, M. Zhang, Multifunctional Triblock Nanocarrier (PAMAM-PEG-PLL) for the Efficient interacellular siRNA Delivery and Gene Silencing, ACS Nano. 5 (2011) 1877–1887.

[22]L. Cui, J. Li, X.-G. Zhang, Preparation and properties of Co_3O_4 nanorods as supercapacitor material, J. Appl. Electrochem. 39 (2009) 1871–1876.

[23]S. Chaturvedi, P.N. Dave, N.K. Shah, Applications of nano-catalyst in new era, J. Saudi Chem. Soc. 16 (2012) 307–325.

[24]A.T. Bell, The impact of nanoscience on heterogeneous catalysis., Science. 299 (2003) 1688–91.

[25]A. a. Ensafi, M. Jafari-Asl, B. Rezaei, a. R. Allafchian, Simultaneous determination of guanine and adenine in DNA based on $NiFe_2O_4$ magnetic nanoparticles decorated MWCNTs as a novel electrochemical sensor using adsorptive stripping voltammetry, Sensors Actuators B Chem. 177 (2013) 634–642.

[26]A. B. P. Lever, Inorganic Electronic Spectroscopy, Elsevier, Amsterdam, 1984.

[27]K. Nakamoto, Infrared and Raman Spectra of Inorganic and Coordination Compounds, Part II: Application in Coordination, Organometallic and Bioinorganic Chemistry, 5th ed, Wiley-Interscience, New York, n.d.

[28]M. Ahrén, L. Selegård, F. Söderlind, M. Linares, J. Kauczor, P. Norman, et al., A simple polyol-free synthesis route to Gd_2O_3 nanoparticles for MRI applications: an experimental and theoretical study, J. Nanoparticle Res. 14 (2012) 1006.

[29]K. Lee, Y. Bae, S. Byeon, Nanowires Science and Technology, InTech, 2010.

[30]R. Jenkins, R.L. Snyder, Introduction to X-ray Powder Diffractometry, John Wiley & Sons, Inc., Hoboken, NJ, USA, 1996.